Nanomaterials have rapidly created a niche in the field of biomedical and pharmaceutical application due to their unique optoelectronics properties [Jain *et al.* (2008), Sayed (2001)]. There is a growing need to minimize the use of toxic chemical substance to synthesize new substance. Gold nanoparticles have emerged as a **star** in the galaxy of noble nanoparticles due to their diversified applicability [Ngo *et al.* (2012), Panda *et al.* (2011), Gangula *et al.* (2011)]. They are being extensively used for diagnostic and therapeutic purposes [Luo *et al.* (2004), Cao *et al.* (2002), Shi *et al.* (2007), Boca *et al.* (2011)].

Various physical and chemical methods used for gold nanoparticle synthesis were stringent due to ecological hazardous and energy consuming [Riabinina *et al.* (2012), Liu *et al.* (2007)]. In case of chemical methods, the adsorption of toxic chemical substances on nanoparticles makes them undesirable for pharmaceutical applications [Parashar *et al.* (2009)]. Therefore, biosynthesis of noble metal nanoparticles has come into limelight. It involves the utilization of biological synthesized non toxic reducing and capping agents [Xie *et al.* (2007)]. Resources like bacteria, algae, fungi, yeast and plant extracts have employed for biogenesis of nanoparticles [Ganesh *et al.* (2009), Schrofel *et al.* (2011), Priyadarshini *et al.* (2013), Montes *et al.* (2011)]. However, fungus has an edge over other microorganisms. It offers easily handling, simple purification and allows feasible scale-up due to the presence of secretary compounds like enzymes in them. [Mukherjee *et al.* (2001)].

Biosynthesis of nanoparticles have been demonstrated by the use of biological agents such as bacteria, fungi, yeasts, actinomycetes and plants. The biological synthesis of nanoparticles from fungi is considered to be significant branch, due to the fungi tolerance and metal bioaccumulation capability. Filamentous fungi species are of particular interest because they are able to produce highly stable NPs, which prevent molecular aggregation

even after prolonged storage, and therefore have improved longevity [Mukherjee P. et. al. (2001)]. Some species including *Verticillium* sp., *Cladosporium cladosporoides*, *Trichoderma asperellum*, and some species of Aspergillus, Penicillium and Fusarium have been successfully used for synthesis of metallic NPs [Ahmad *et al.* (2002), Balaji *et al.* (2009), Bhainsa *et al.* (2006), Duran *et al.* (2005), Li *et al.* (2008), Mouxing *et al.* (2006), Mukherjee *et al.* (2001), Swetha *et al.* (2013)].

The present work is aimed to understand the role of the electrochemical behavior of various mold strains in gold nanoparticle formation. The gold salt was converted into gold nanoparticles by different mold strains, viz. *Aspergillus flavus* NCIM650, *Phoma exigua* NCIM 1237, *Aspergillus niger* NCIM 616, *Aspergillus niger* NCIM 1025 and *Trichoderma reesei* NCIM 992. The synthesized gold nanoparticles were characterized using UV-Visible spectral analysis & Transmission electron microscope (TEM). The applicability of the synthesized gold nanoparticles were tested to suitable antioxidant using the DPPH assay and Hydrogen Peroxide assay.

4.1 Strains Selected

Six microbial strains were acquired from National Collection of Industrial Microorganisms (NCIM), National Chemical Laboratory (NCL), Pune, India.

Mold Species

1) *Aspergillus flavus* NCIM650
2) *Phoma exigua* NCIM1237
3) *Aspergillus niger* NCIM 616
4) *Aspergillus niger* NCIM 1025
5) *Trichoderma reesei* NCIM 1186
6) *Trichoderma reesei* NCIM 992

Conversion of Gold Chloride salt into Gold Nanoparticles

The Au^{3+} reduction, by any reducing agent to Au^0 takes place via a number of redox reactions. When the reducing agent is introduced into the aqueous $HAuCl_4$ solution, electrons are donated to the $[AuCl_4]^-$ ions. For $[AuCl_4]^-$ ions to be reduced to gold atoms, a series of redox reactions take place. This includes the liberations of Cl^- ions and is described by Equations 2 and 3.

$$AuCl_4^- + 2e- \rightarrow AuCl_2^- + 2Cl^- \quad (4)$$

$$AuCl_2^- + 2e- \rightarrow Au^0 + 2Cl^- \quad (5)$$

The Au^{3+} reduction, by any reducing agent to Au^0 takes place via two redox reactions. This includes the liberations of Cl^- ions and is described by Equations 4 and 5.

4.2 Optimization of Growth Patterns

Cell pellets from each of the identical flasks was emptied at regular time intervals and packed cell volume (PCV) was measured. It is used for the study of growth pattern of mold.

Growth Characteristic of *Aspergillus flavus* NCIM 650

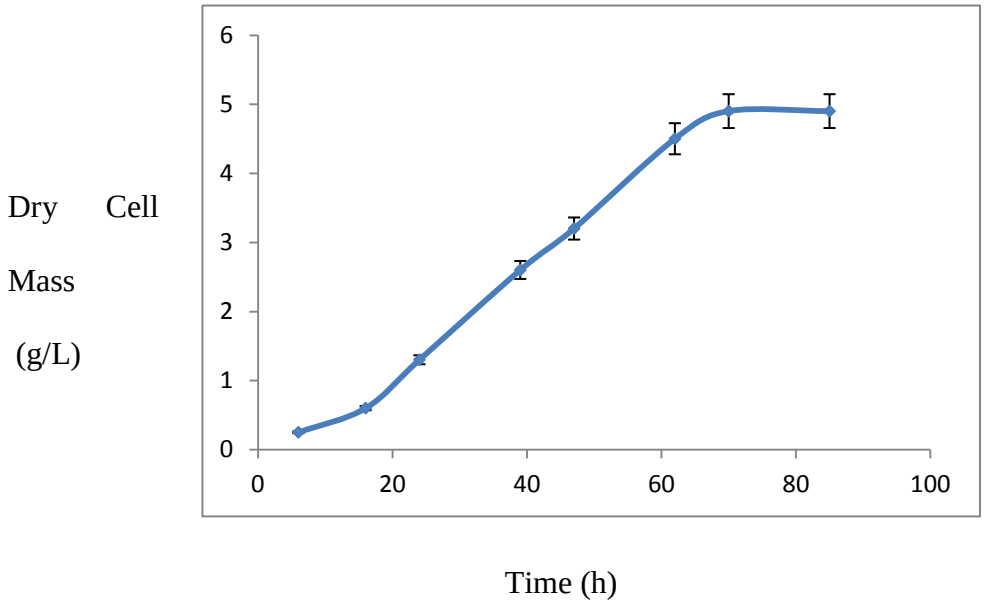

Figure 4.1: Characteristic growth curve of *Aspergillus flavus* NCIM 650

Growth Characteristic of *Aspergillus niger* NCIM 616

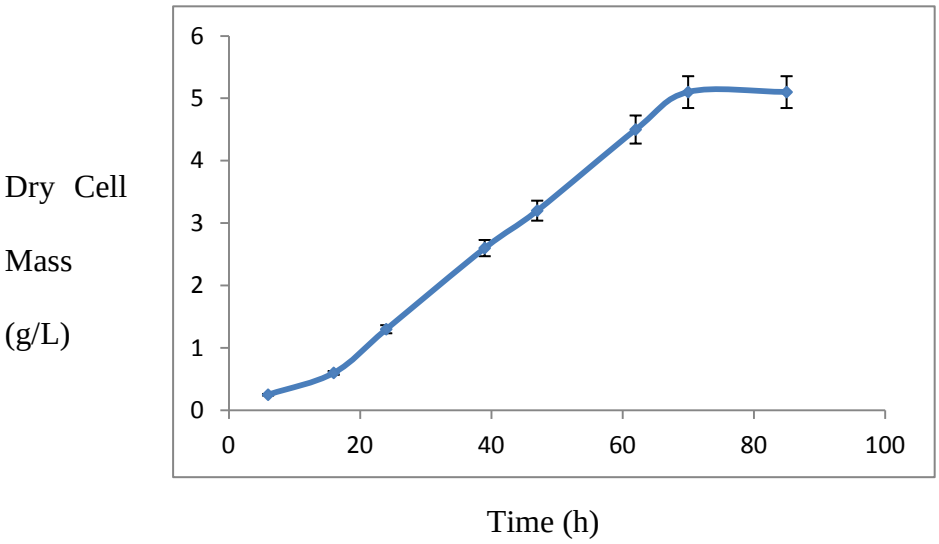

Figure 4.2: Characteristic growth curve of *Aspergillus niger* NCIM 616

Growth Characteristic of *Aspergillus niger* NCIM 1025

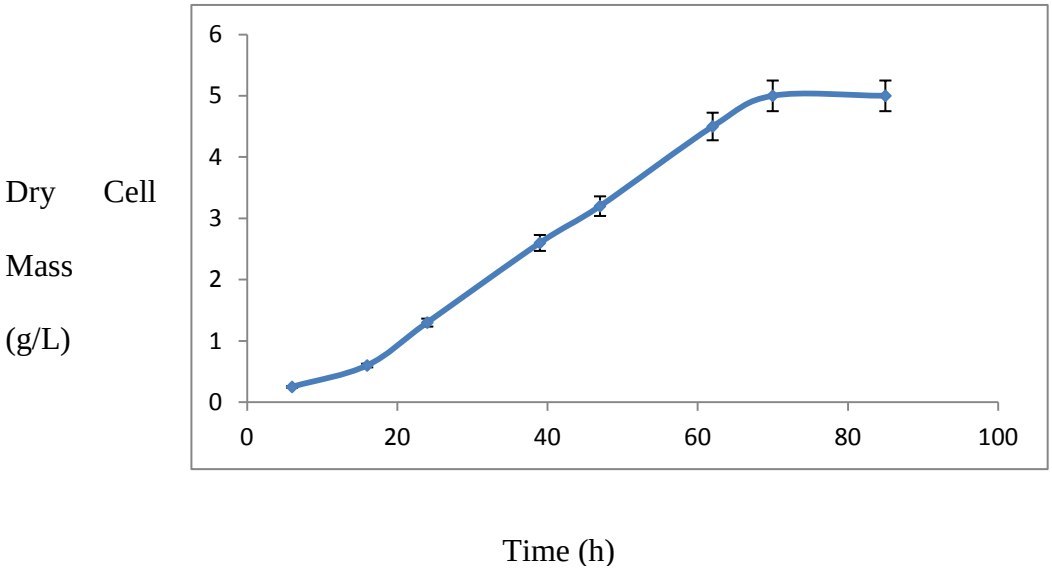

Figure 4.3: Characteristic growth curve of *Aspergillus niger* NCIM 1025

Growth Characteristic of *Phoma Exigua* NCIM 1237

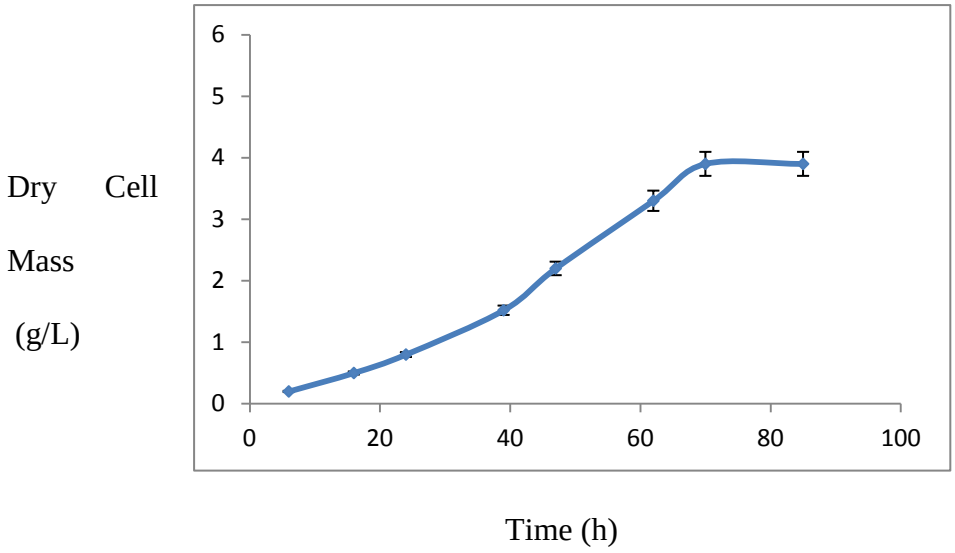

Figure 4.4: Characteristic growth curve of *Phoma exigua* NCIM 1237

Growth Characteristic of *Trichoderma reesei* NCIM 1186

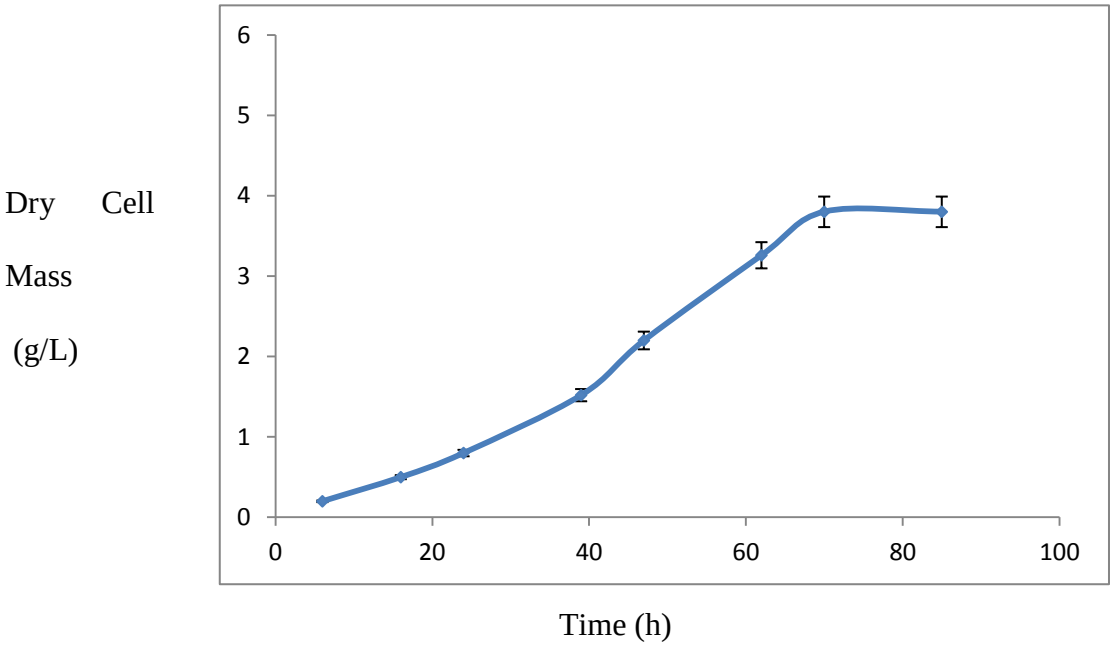

Figure 4.5: Characteristic growth curve of *Trichoderma reesei* NCIM 1186

Growth Characteristic of *Trichoderma reesei* NCIM 992

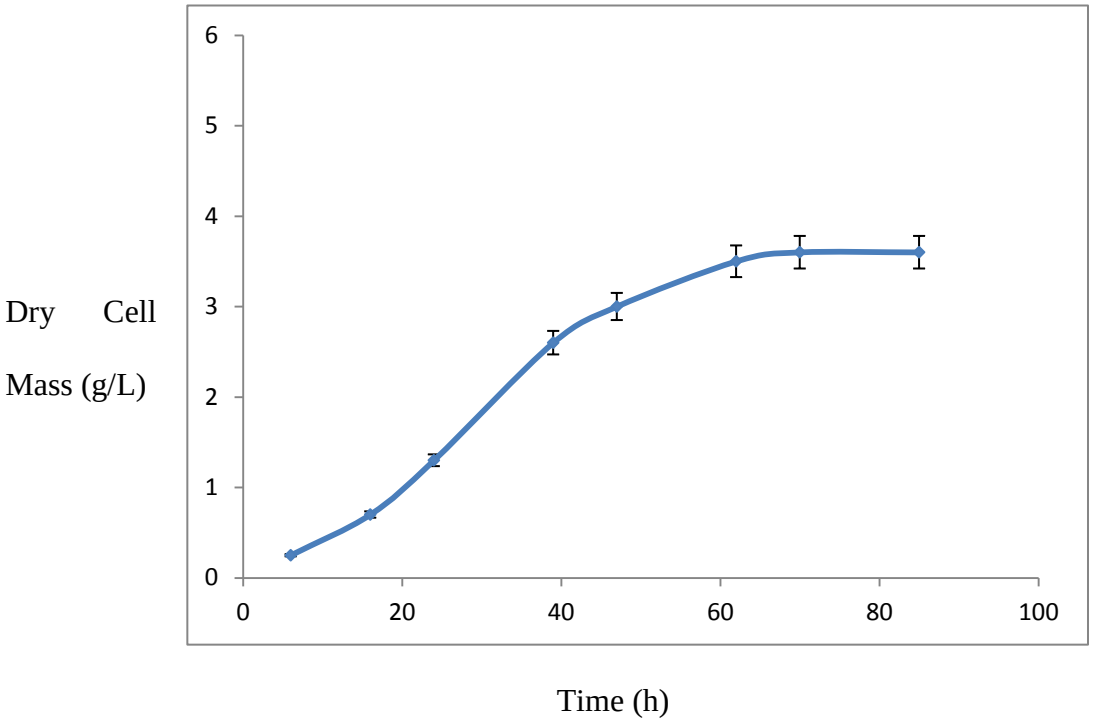

Figure 4.6: Characteristic growth curve of *Trichoderma reesei* NCIM 992

In almost every plot is showing that optimum growth occurs in 70 hours.

4.3 Growth characteristic comparison of control and experimental media (with Gold chloride) for different Molds

The growth characteristic pattern were studied for the species in order to know the effects of gold chloride on the growth pattern of mold species. It was clearly observed in Fig 5.7 that the molds however showed some limited growth and also colour change in biomass in the media, signified the reduction of gold is taking place. So, it can be inferred that there can be two processes of colloidal gold nanoparticles; one is that we can produce the conventional biomass first and then we can incubate with gold chloride or, the secondly we can grow the cell mass directly with gold chloride.

Both the process has got their advantages, like if we grow the biomass first and then gold chloride incubation is done, we can have more amount of gold nanoparticles per gram of gold chloride reduced, but it's a long process, whereas in contrast, through the amount of gold nanoparticles produced is low, but the process is quicker and involves less labor.

So, it's the requirement criteria, which will force the process to be used and which are not to be used. But if one can design, or grow a mutant strain which has high tolerability to gold, growing it directly with added gold chloride, then its assured to be a revolution in speedy production and recovery of the nanoparticles.

Growth pattern of the various mold strains were studied both in normal nutrient media as well as in the presence of gold chloride to analyze the effect of salt on the growth of mold strains. In the presence of gold chloride, there was decrease in growth, as compared to normal growth pattern. It was due to inhibitory effect of gold chloride on the mold growth. The limited growth is associated with the reduction of the salt. Due to this, the mold biomass acquired a faint bluish colour and media turned pinkish in colour. Growth associated nanoparticle reduction is not very efficient as shown. Therefore, it is economical and beneficial to grow the biomass first and then incubating in gold chloride.

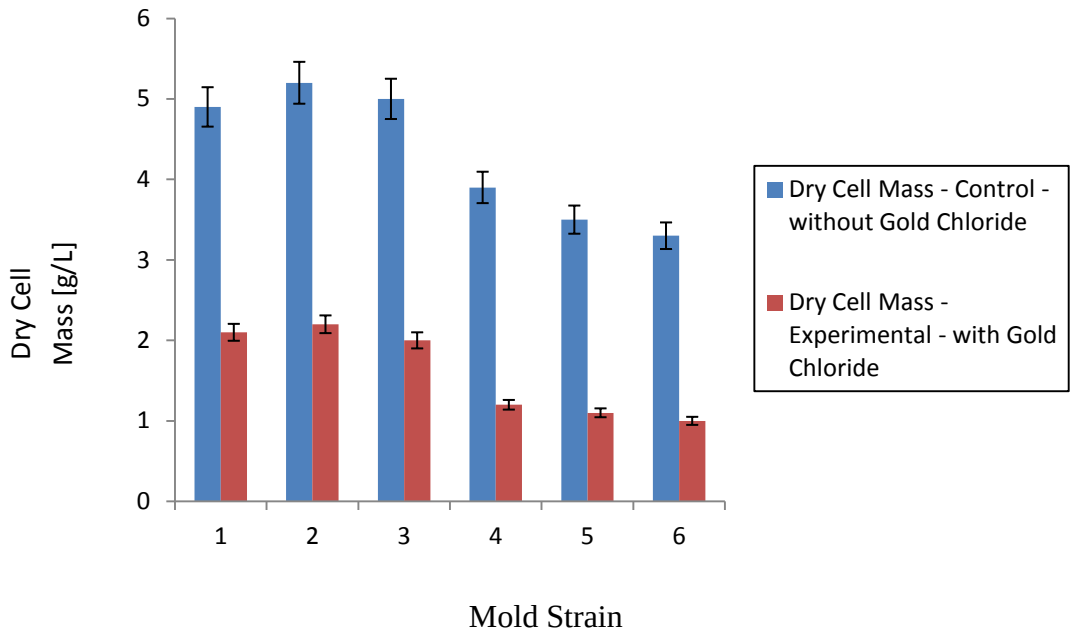

Fig. 4.7: Comparative bar chart for growth pattern of two different mold strains i.e. without and with gold chloride solution of different Mold strains

[Strain 1 = *Aspergillus flavus* NCIM 650; Strain 2 = *Aspergillus niger* NCIM 616; Strain 3 = *Aspergillus niger* NCIM 1025; Strain 4 = *Phoma exigua* NCIM 1237; Strain 5 = *Trichoderma reesei* NCIM 1186; Strain 6 = *Trichoderma reesei* NCIM 992]

During the growth study, highest growth occurs in *Aspergillus niger*. So, *Aspergillus niger* is better among six. Of the two strains *Aspergillus niger NCIM* 616 and *Aspergillus niger NCIM* 1025, *Aspergillus niger* NCIM 616 is better.

During the growth study, lowest growth occurs in *Trichoderma reesei*. *Trichoderma reesei* is best among six. Lesser the growth, lesser will be the toxic effect of the salt. Of the two strains *Trichoderma reesei* NCIM 1186 and *Trichoderma reesei* NCIM 992, *Trichoderma reesei* NCIM 992 is better.

4.4 Cyclic Voltammetry Studies of Molds

Mold strains showed excellent pellet formation at the end of the aerobic phase. Filtered culture media did not show any significant peak for any of the strains. This indicates that under normal conditions, the mold strains have no inclination towards redox mediators. The Emediator values vs. NHE of *Aspergillus flavus* NCIM 650, *Aspergillus niger* NCIM 616, *Aspergillus niger* NCIM 1025, *Phoma exigua* NCIM 1237 and *Trichoderma reesei* NCIM 992 were found to be 0.366V, 0.381V, 0.355V, 0.3V and 0.233V respectively. The measured reduction potentials as shown in (Fig. 4.8 to 4.12) suggest that these microorganisms have potential for reducing metal ions with higher reduction potential such as gold metal salt (E_0 = +1.50 V). In anaerobic conditions, the metal ions present in media with higher reduction potential can effectively serve as electron acceptors instead of oxygen.

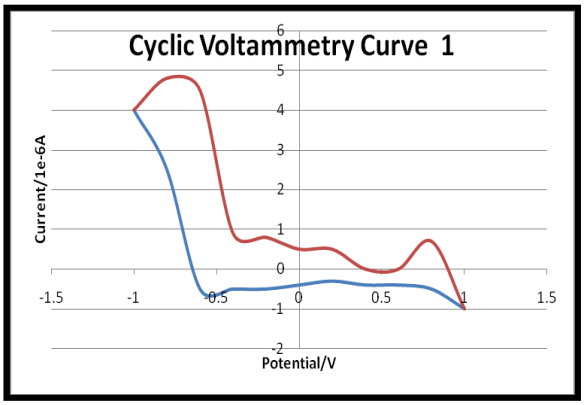

Figure 4.8: Voltammogram curve for blank media

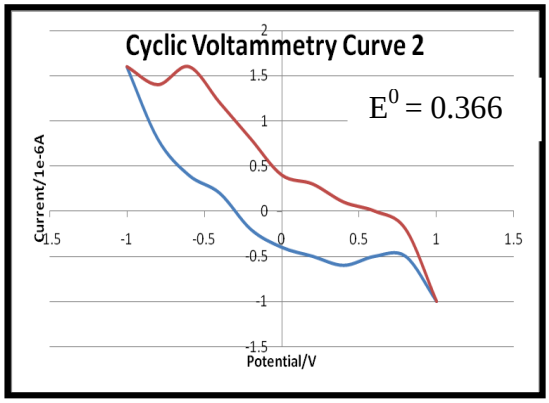

Figure 4.9: Voltammogram curve for *Aspergillus flavus* NCIM 616

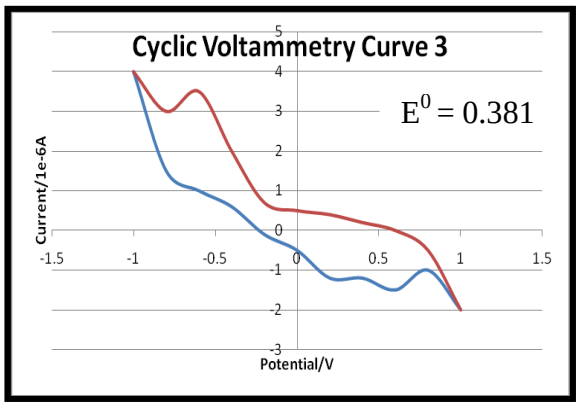

Figure 4.10: Voltammogram curve for *Aspergillus niger* NCIM 616

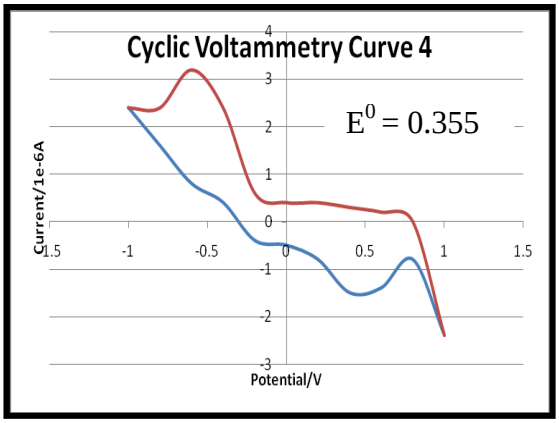

Figure 4.11: Voltammogram curve for *Aspergillus niger* NCIM 1025

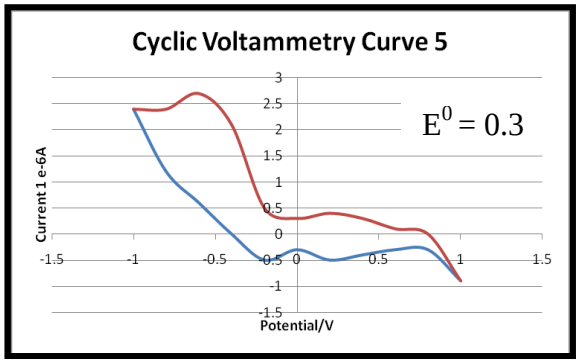

Figure 4.12: Voltammogram curve for *Phoma exigua* NCIM 1237

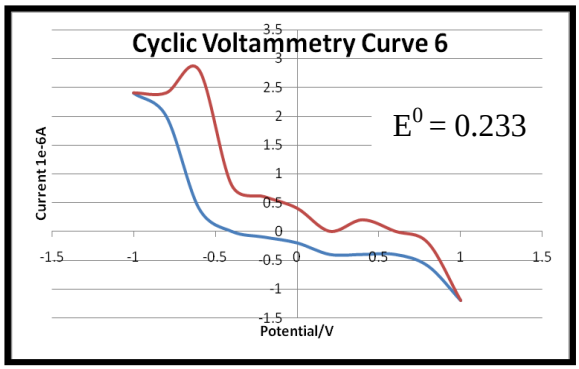

Figure 4.13: Voltammogram curve for *Trichoderma reesei* NCIM 992

Significant peaks were observed in *Aspergillus niger* NCIM 616 & *Aspergillus niger* NCIM 1025, for cultures grown in gold chloride supplemented media. For *Aspergillus flavus* NCIM 650 & *Phoma exigua* NCIM 1237, only test condition induces mediator release. The presence of small peak in case of *Trichoderma reesei* indicated that highest reduction capacity.

These strains have a natural tendency towards mediator release when soluble electron acceptor species are present in the media. The results suggests that in the absence of oxygen as electron acceptor for the completion of the electron transport chain, the mold strains are capable of releasing soluble electron mediators to utilize the other possible electron acceptor present in the media. Formation of noble metal nanoparticles took place when the

microorganisms are cultured with noble metal ions in anaerobic conditions. The process of metal reduction could take place as the mediators formed by the microorganisms have lower reduction potential than the metal ions present in the solution making them strong reducing agents.

Standard Reduction Potential (E^0) of Gold salt [Au(III)/Au(0)] is +1.50 and Silver salt [Ag(I)/Ag(0)] is +0.799. As lesser the E^0, more stronger is the reducing agent. Since E^0 value of *Trichoderma reesei* NCIM 992 is lowest, so it is strongest reducing agent among others.

4.5 Synthesis of Gold Nanoparticles from different Molds

Slants and plates was prepared for mold culture. The master slant of Molds were first reviewed in their subsequent media and sub-cultured in freshly prepared slants for the experiments. The master slant was refrigerated at 4°C for future purpose and reference [Barua *et al.* (2015)].

Mold strains were inoculated in 100 ml of Czapek Dox Broth Media at 28ºC and incubated 200 rpm in a shaker incubator. After three days of incubation, the mycelium was separated by filtration and washed thrice with Milli-Q deionized water. The biomass was supplemented with 1 ml of 10 mM $HAuCl_4$ (prepared in deionized water) and incubated at 200 rpm in anaerobic condition at 28°C for 24 hours and the colour changes were observed. Simultaneously, a positive control of incubating the mold mycelium with deionized water and a negative control containing only gold chloride solution were maintained under same conditions. The samples were removed for nanoparticle characterization. After the removal of samples for nanoparticle characterization, the cultures were left in incubation to determine the effect of extended incubation periods.

a **b**

Figure 4.14**:** Formation of Gold Nanoparticles (a) Control (b) Gold Nanoparticles, in solution

The amount of Gold Nanoparticles produced was measured using Inductively Coupled Plasma Mass Spectrometry (ICP-MS). ICP-MS of the residual Gold Chloride salt revealed that more than 75% of the Gold Chloride salt was converted to nanoparticles as shown in **Table 4.1**.

Table 4.1: ICP-MS of the Residual Gold Chloride Salt

Metal Salt	**Original Salt Concentration**	**Residual Salt Concentration**	**Percentage of Bioreduction of Silver Nitrate Salt**
Gold Chloride Salt	70 ppm	12.5	82.1

4.6 Characterization of Gold Nanoparticles

4.6.1 Biotransformation (Surface Plasmon Resonance) and UV-Vis Spectral studies

A. Aspergillus flavus NCIM 650

On the addition of gold chloride solution, a faint pink colour was developed after one hour. At the end of 24 hours, media colour was deep pink. Sonication of samples depend the media colour indicating a reduction of gold salt had occurred mostly extracellular. By the second day, pellets turned pink and colour deepened to form deep purple colour over the next two days.

B. *Aspergillus niger* NCIM 616

On the addition of Gold Chloride solution, colour change was observed within 30 minutes. The colour developed was initially faint pink that deepened over a period of 24 hours. Sonication of samples collected at this point did not affect the media colour considerably, indicating an extracellular reduction of gold salt, which is in accordance with the Cyclic Voltammetry (CV) results. The media colour faded over the next two-three days to the final light purple colour. The fungal pellets acquired a faint pink colour.

C. *Aspergillus niger* NCIM 1025

On addition of gold chloride solution, colour changes was observed within 30 minutes. The pink colour changed to violet within 24 hours. Sonication of samples deepened the media colour slightly. Most of the reduction had occurred extracellular, in accordance with the Cyclic Voltammetry (CV) results. The media colour faded over the next two-three days to a final colourless condition and the fungal pellets acquired a bluish-black colour.

D. Phoma exigua NCIM 12137

On addition of gold chloride solution, a faint pink colour was observed after one hour. At the end of 24 hours, the pellets had acquired a deep blackish blue colour. Sonication of samples not deepened the media colour, indicating a reduction of gold salt had occurred

intracellularly. The media colour persisted for two days and then gradually faded to colourless.

E. Trichoderma reesei NCIM 1186

Pink colour of media was observed after 24 hours of incubation. Sonication of the sample led to increasing the colour intensity. By the end of third day, the pellets acquired a deep black colour.

UV-Vis. Spectroscopy study of the lightly sonicate samples for the Surface Plasmon Resonance showed peaks which is based on the particle sizes of Gold Nanoparticles. It varies between 5 – 100 nm, as the value of peak wavelength changes between 515 – 572 nm, which is characteristic of gold nanoparticle. Similarly, the absorbance of Gold Nanoparticle solution measured at a wavelength of Surface Plasmon peak and its intensity varied with the mold strains, indicating the possible differences in Gold Nanoparticle size and morphology.

The UV-Vis. Spectra of blank Czapek Dox Broth media supplemented with Gold Chloride did not shows any contribution. The Surface Plasmon peak for Gold nanoparticles produced by *Aspergillus flavus* NCIM 650, *Aspergillus niger* NCIM 616, *Aspergillus niger* NCIM 1025, *Phoma exigua* NCIM 1237, *Trichoderma reesei* NCIM 1186 and *Trichoderma reesei* NCIM 992 were recorded as 536 nm, 543 nm, 542 nm, 560 nm, 537 nm & 528 nm respectively (Figure 5.15 – 5.21). The spectral shift accompanied by broadening of the Surface Plasmon Resonance could be attributed to the increment in gold nanoparticle size [Kumar *et al.* (2008), Njoki *et al.* 2007].

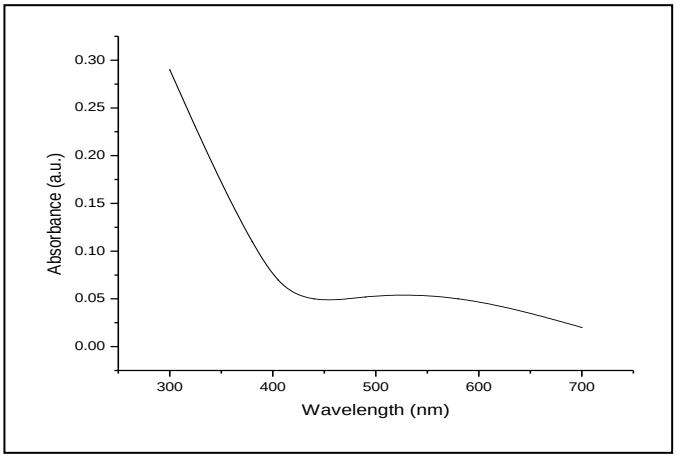

Figure 4.15: UV-Visible spectra of Blank media

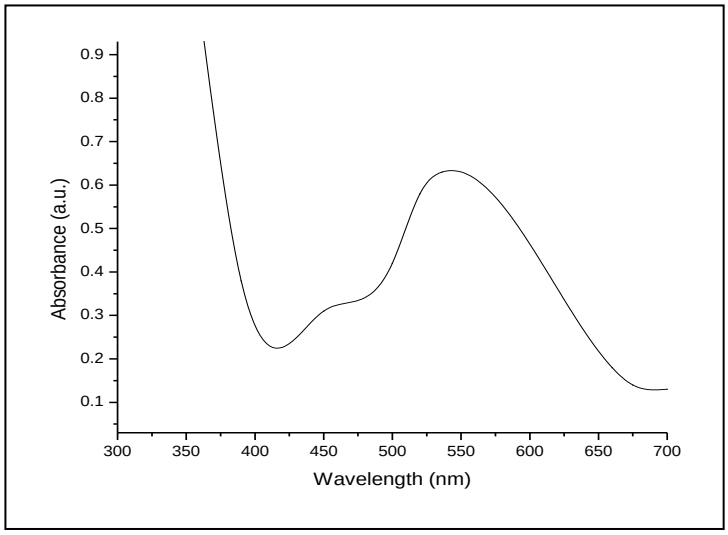

Figure 4.16: UV-Visible spectra of Gold Nanoparticles prepared by *Aspergillus flavus* NCIM 650

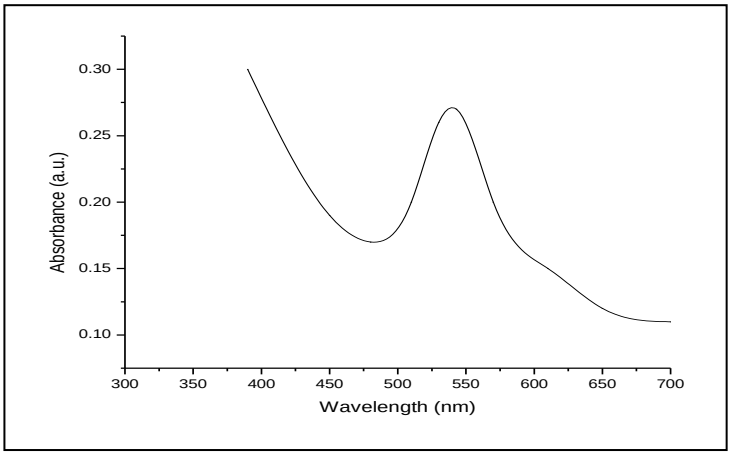

Figure 4.17: UV-Visible Spectra of Gold Nanoparticles prepared by *Aspergillus niger* NCIM 616

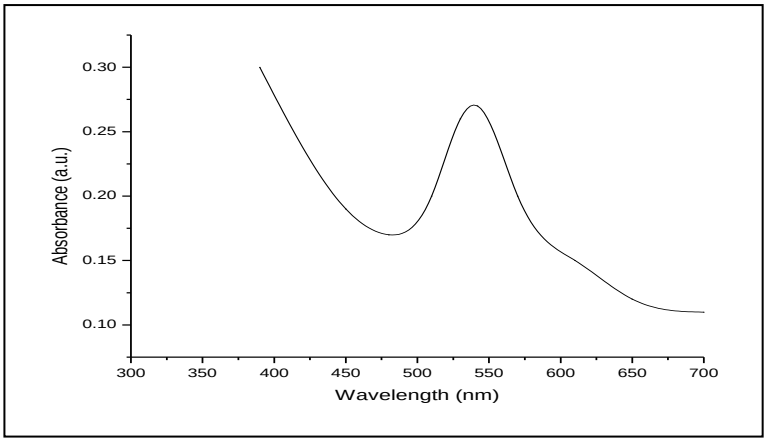

Figure 4.18: UV-Visible Spectra of Gold Nanoparticles prepared by *Aspergillus niger* NCIM 1025

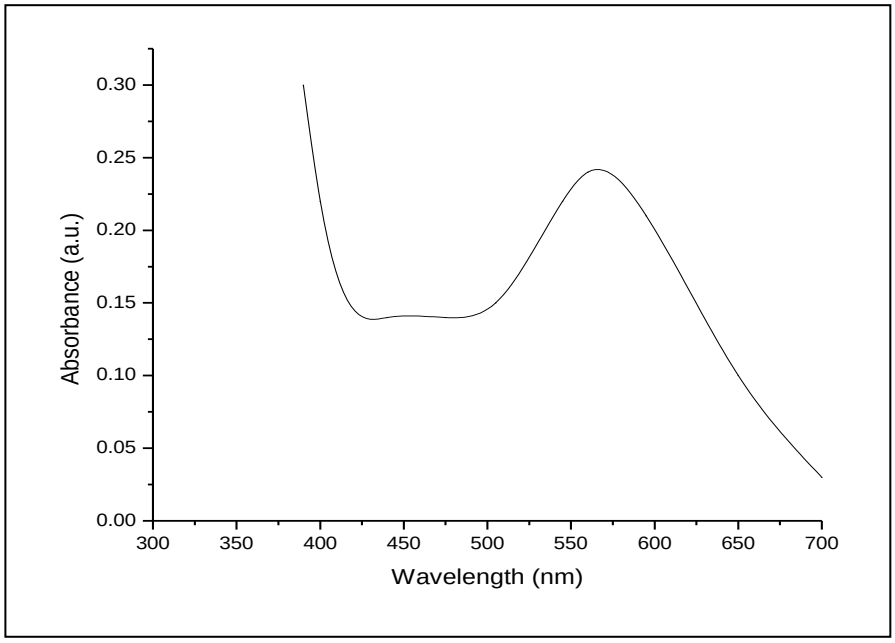

Figure 4.19: UV-Visible Spectra of Gold Nanoparticles prepared by *Phoma exigua* NCIM 1237

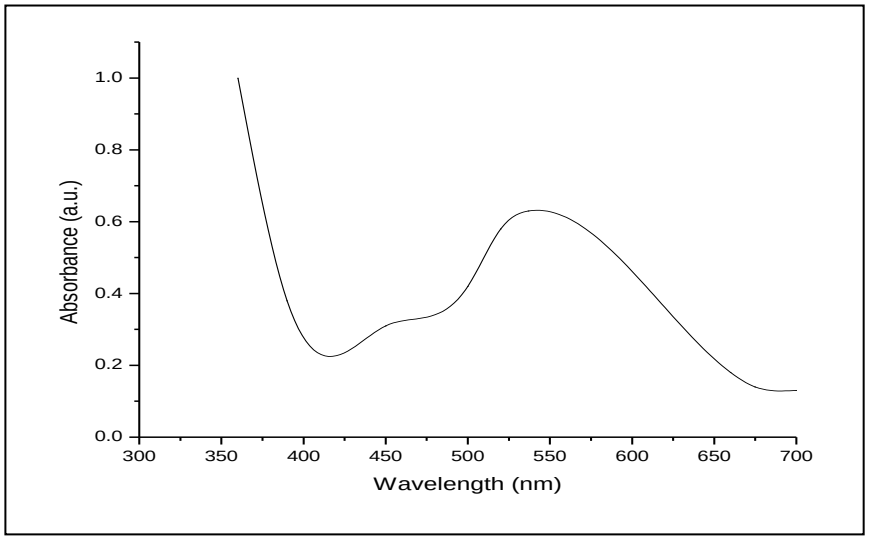

Figure 4.20: UV-Visible Spectra of Gold Nanoparticles prepared by *Trichoderma reesei* NCIM 1186

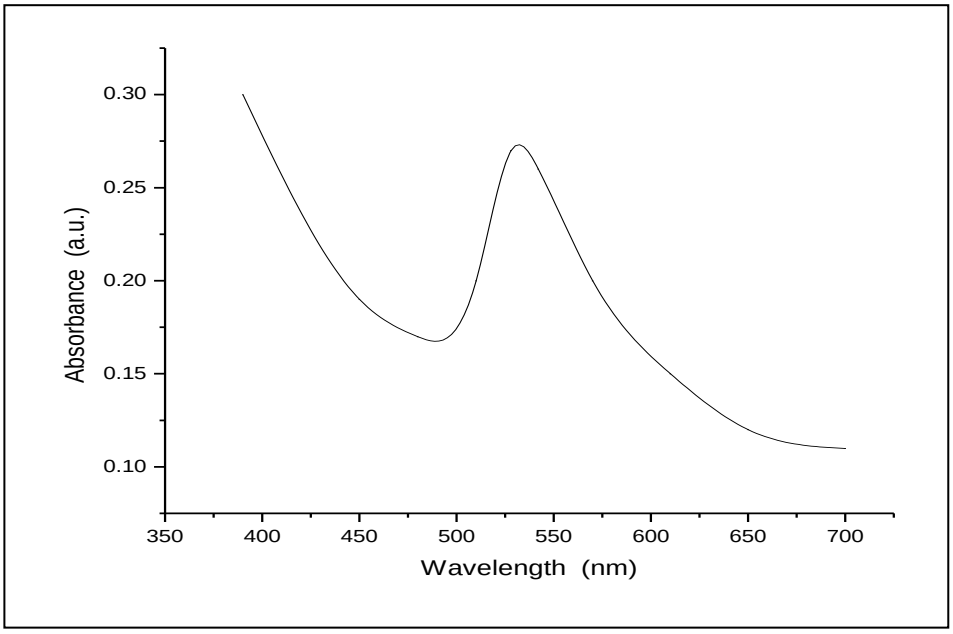

Figure 4.21: UV-Visible Spectra of Gold Nanoparticles prepared by *Trichoderma reesei* NCIM 992

4.6.2 Fourier Transform Infrared Spectroscopy (FTIR) Studies of Gold Nanoparticles

Best strain was characterized as *Aspergillus niger*. FTIR measurements were carried out to identify the possible (protein) bio-molecules responsible for the capping and efficient stabilization of the metal nanoparticles synthesized by *Aspergillus niger*. FTIR studies were conducted to determine the various chemical functional groups present in the sample containing the nanoparticles. FTIR spectra of untreated mold biomass and mold biomass supplemented with gold metal salts were shown in Figure 4.22 and 4.23.

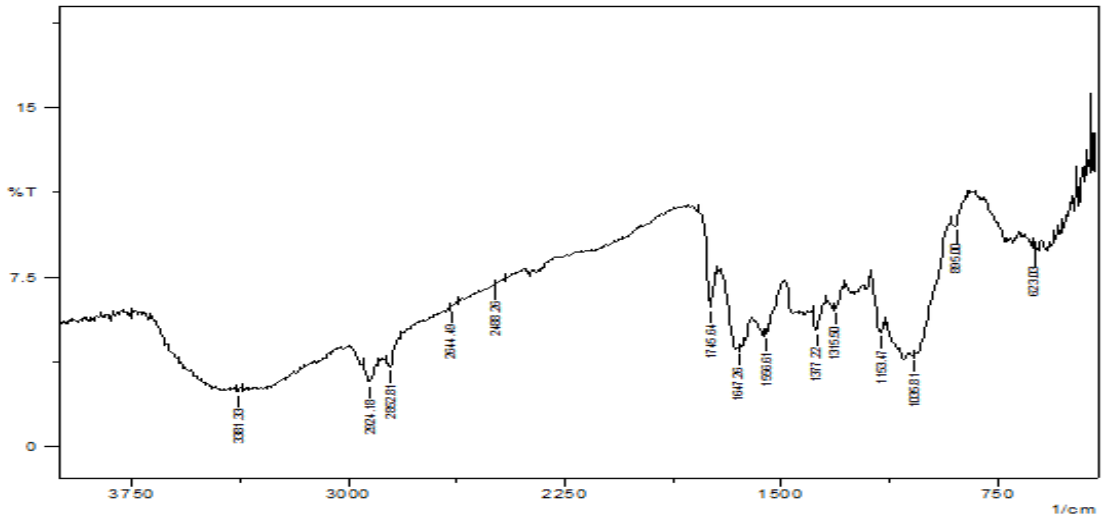

Figure 4.22: FTIR Spectra of lyophilised Mold biomass

The bioreduced chloroauric acid solution was centrifuged at 15,000 rpm for 15 min, and the pellet was washed with deionized water to get rid of the free proteins/enzymes that were not capping the gold nanoparticles. Thereafter, the purified suspension was freeze-dried to obtain dry powder. The dried powder was analysed using FTIR.

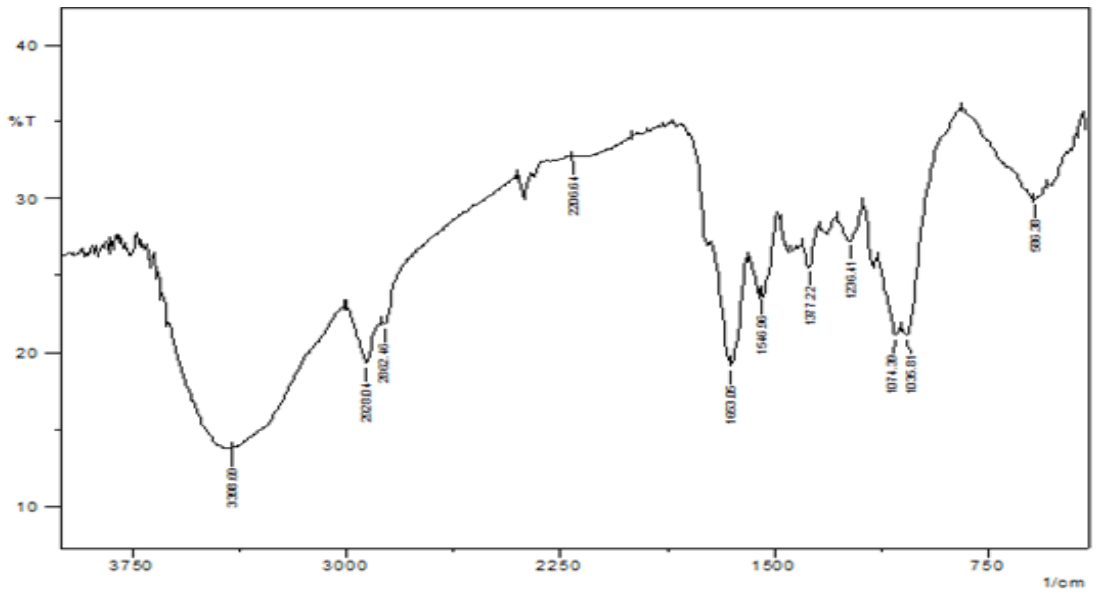

Figure 4.23: FTIR spectra of Mold biomass treated with Gold salt

The FTIR results of the *Aspergillus* with and without Gold Chloride additions is depicted in the above graph. The broad band contour that appears in the range of 3000-3400cm^{-1} [3381 and 3386 cm^{-1}] is due to the association of intermolecular Hydrogen bonds arising from NH_2 and OH groups which becomes broader after reacting with Gold ions. Infrared active modes attributed to side chain vibrations include C-H stretching anti-symmetric and symmetric modes at 2924 and 2928 cm^{-1} corresponding to aliphatic and aromatic modes that broaden only after reacting with gold solution.

The bands observed at 1377 cm^{-1} can be assigned to the C-N stretching vibrations of aromatic and aliphatic amines. The aromatic amine band gets less intensified in gold nanoparticles formed after the reaction. The significant changes observed at 1377 cm^{-1} is indicative of the role of aromatic groups in reduction of Au ions in Au/mycelium which possibly arise from aromatic amino acids tryptophan or tyrosine. The peaks at around 1036 cm^{-1}, 1074 cm^{-1} in the C–O stretching vibrating region, are indications of gold ions interactions with the fungal protein of mycelium. The spectrum showed peaks at 623 cm^{-1} due to C-Cl stretching and 586 cm^{-1} due to C-Br stretching of alkyl halide.

4.6.3 Particle Size Analysis of Gold Nanoparticles

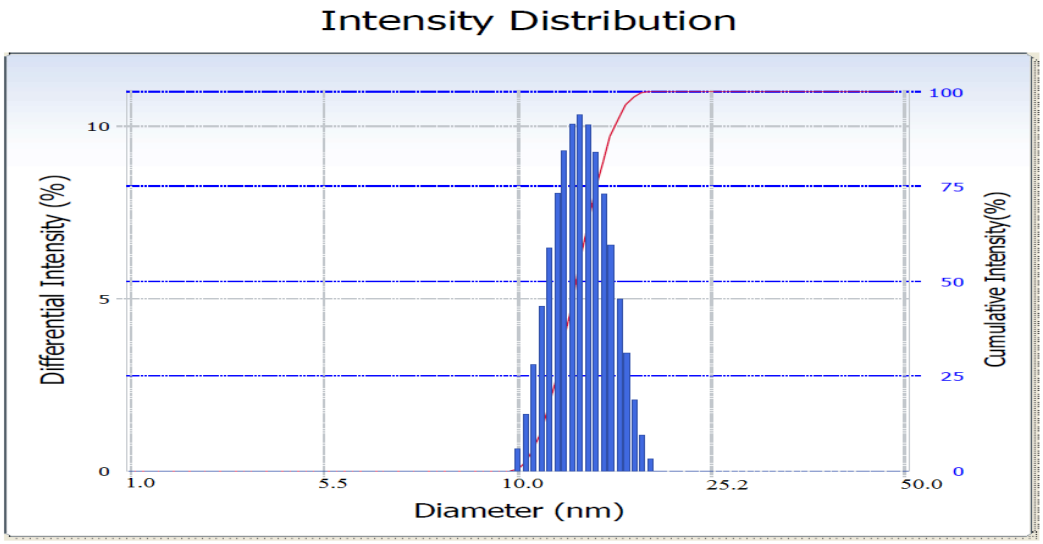

Figure 4.24: Particle Size of Gold Nanoparticles

- Size range of Gold Nanoparticle 10-20nm

4.6.4 Scanning Electron Microscopy – Energy Dispersive X-Ray (SEM-EDX) Analysis of Gold Nanoparticles

The structural features of the produced gold nanoparticles were characterized using SEM. As the metal particles are good conductors, they can be observed without any prior carbon coating at a magnification of 1000× in a voltage of 10 kV. Fig. 5.25 is the SEM image of *Aspergillus niger* biomass after the addition of the chloroauric acid at 1-100 nm. It was identified from SEM images that the mold mycelia loaded with glittering particle. This depicts that the glittering particles on the mycelia should be gold nanoparticles accumulated on the mycelia intracellularly. The gold nanoparticles loaded in the mycelia were found to be in the size range of 85.1-100 nm.

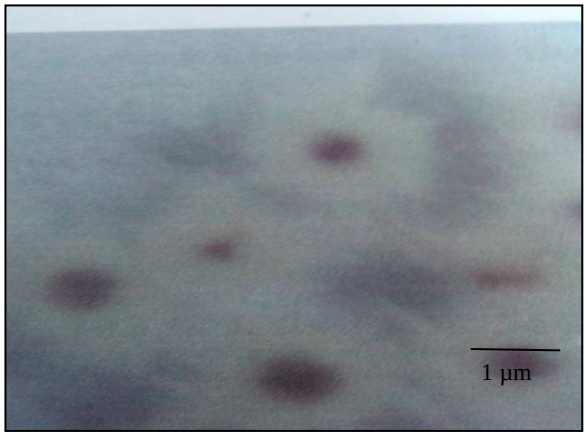

Figure 4.25: SEM image of Gold Nanoparticles prepared by *Aspergillus flavus* strain

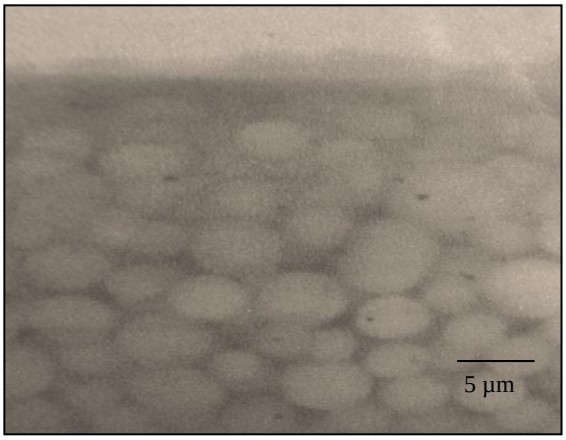

Figure 4.26: SEM image of Gold Nanoparticles prepared by

Aspergillus niger NCIM 616 strains

The average nanoparticle size lies in the range of 50–60 nm. Figure 4.28 shows the harvested AuNPs isolated from the cell mass of *Phoma exigua*

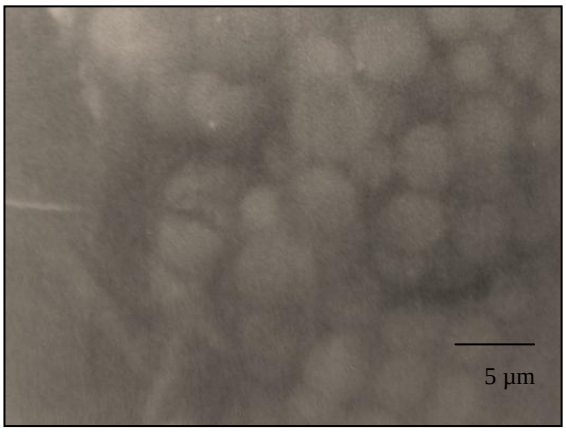

Figure 4.27: SEM image of Gold Nanoparticles prepared by

Aspergillus niger NCIM 1025

Scanning electron microscope (SEM) images show formation of AuNPs on the mycelia surface, suggesting mycelia acts as a template in the AuNP synthesis. On the mycelia surface, AuNPs appeared as bright dots, which is more evident in the high-magnification

image, due to their electron dense metallic character. The average nanoparticle size lies in the range of 60–80 nm. Figure 5.29 shows the harvested AuNPs isolated from the cell mass of *Trichoderma reesei*.

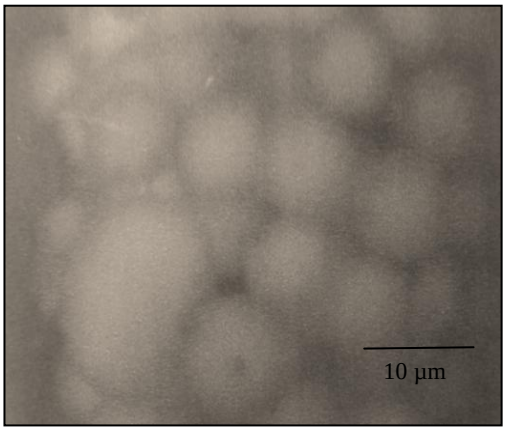

4.28: SEM image of Gold Nanoparticles prepared by

Phoma exigua strain

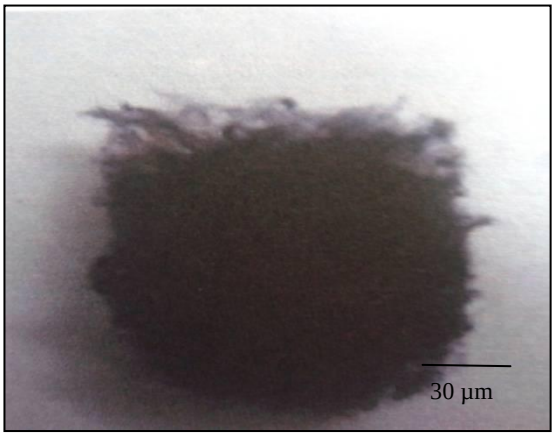

Figure 4.29: SEM image of Gold Nanoparticles prepared by

Trichoderma reesei strains

Energy Dispersive X-ray (EDX) Micrographs of Gold Nanoparticles

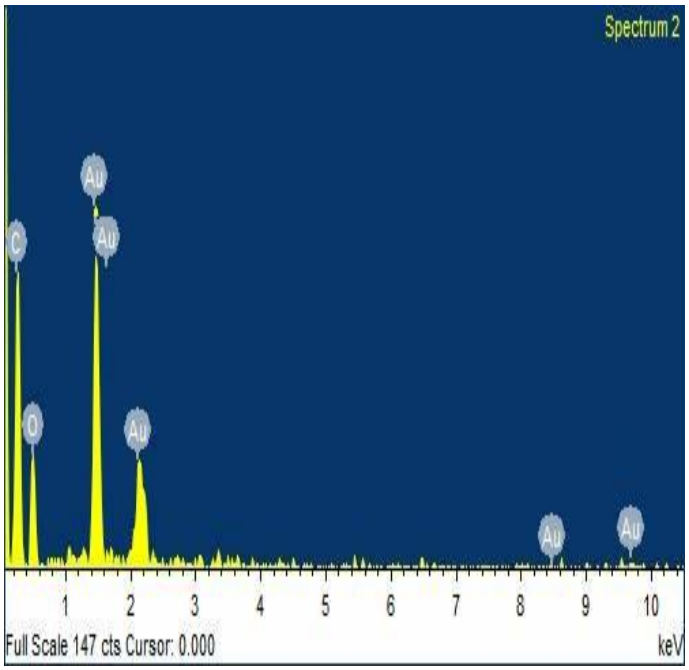

Fig. 4.30: EDX Micrograph of Gold Nanoparticles

SEM images concludes that the nanoparticles were identified from shiny particle on the surface of mold cells. The shiny particle observed to be with no definite morphology.

EDX shows that Carbon and Oxygen peaks attribute to the bio-molecules that are bound to the nanoparticles which are acting as stabilising agents. Peaks of Gold in the EDX spectrum appeared around 1.5-3 keV indicating the existence of gold atoms.

4.6.5 Transmission Electron Microscopy (TEM) Analysis of Gold Nanoparticles

Transmission Electron Microscopy study shown in (figure 5.31 – 5.35) confirm that gold nanoparticles *Aspergillus niger* (both strains) and *Aspergillus flavus* were ranged between 10-20 nm size. The homogeneity in nanoparticles was evident in case of gold nanoparticles produced by *Aspergillus niger* NCIM 616. The nanoparticles synthesized by *Phoma exigua* and *Trichoderma reesei* were quite bulky. They showed agglomerations (23-50 nm) and non-uniformity conspicuously. TEM confirmed the formation of round irregular shape gold nanoparticles.

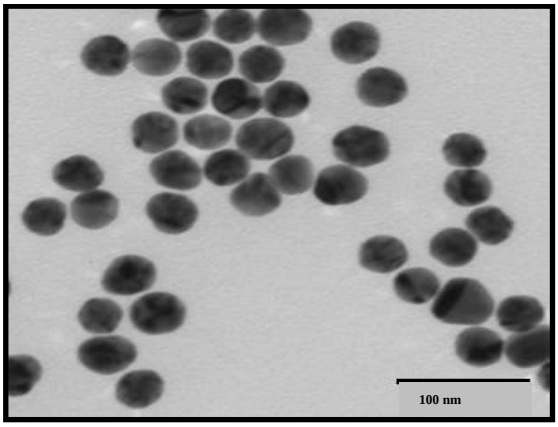

Figure 4.31: TEM image of Gold Nanoparticles obtained from *Aspergillus flavus*

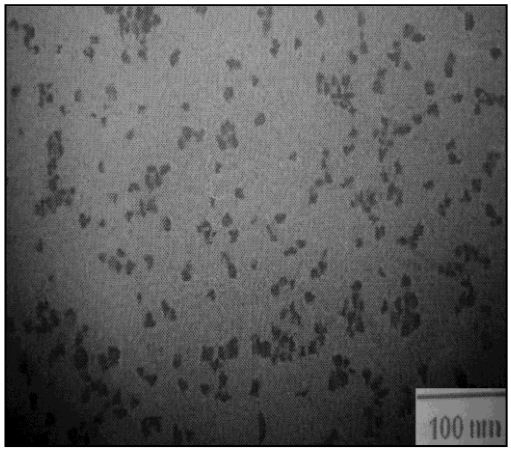

Figure 4.32: TEM image Gold Nanoparticles obtained from

Aspergillus niger NCIM 616

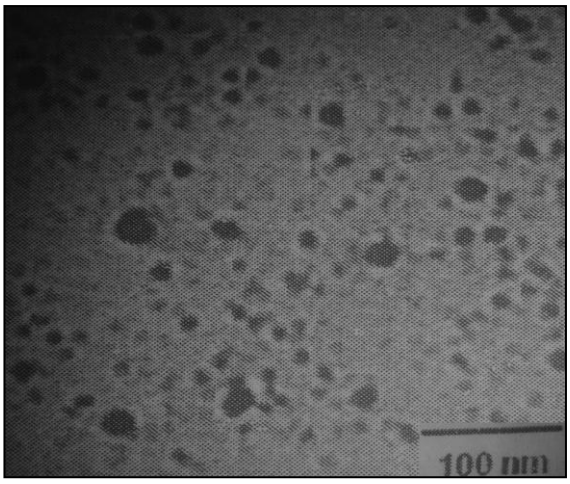

Figure 4.33: TEM image of Gold Nanoparticles obtained from

Aspergillus niger NCIM 1025

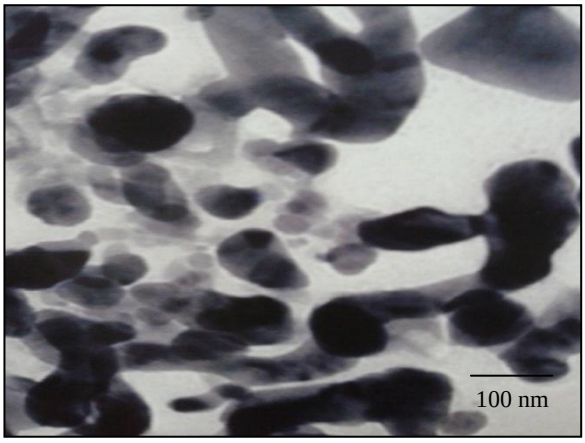

Figure 4.34: TEM image of Gold Nanoparticles obtained from

Phoma exigua

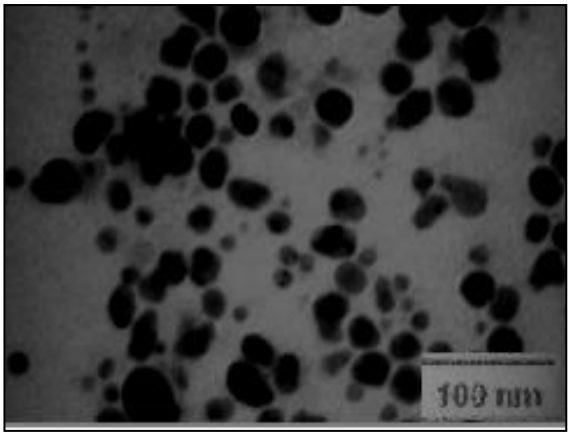

Figure 4.35: TEM image of Gold Nanoparticles obtained from

Trichoderma reesei

4.7 Evaluation of Anti-Oxidant Activities of Gold Nanoparticles (Fabricated by *Aspergillus niger* NCIM 616)

Free radicals are unstable molecules that are known to cause damage to the human body. Damage caused by free radicals is believed to lead to certain types of cancer. Antioxidants are substances that can bond with and stabilize free radicals helping to prevent the damage they cause to the body, thereby reducing the risk of cancer.

Free radical molecules do not have a complete electron shell which makes them more likely to react chemically to nearby molecules which can cause damage to the adjoining cells. One of the most common free radicals encountered by humans is oxygen. The oxygen molecule becomes radicalized when it become electrically charged. Antioxidants neutralize the electrical charge of free radicals.

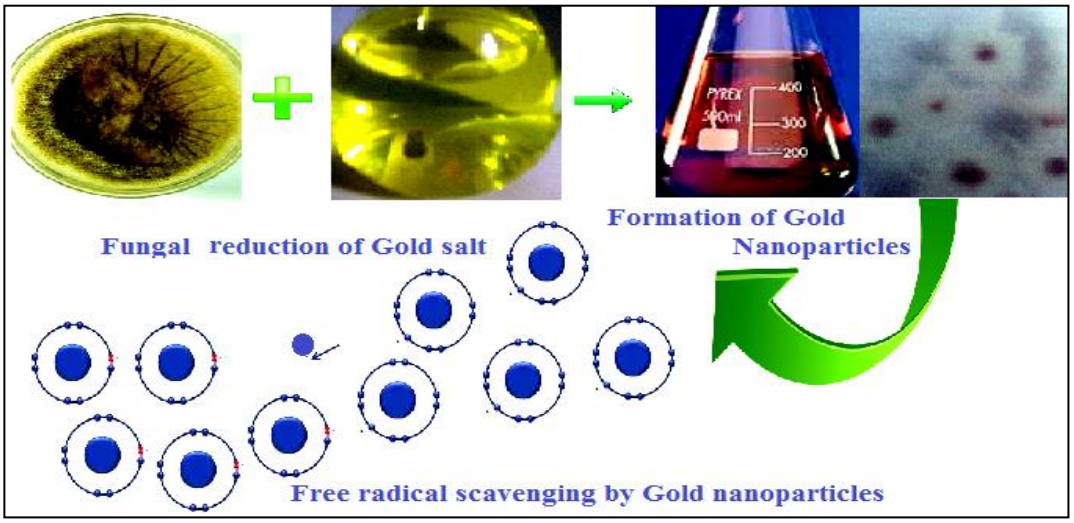

Figure 4.36: Free radical scavenging activity of Gold Nanoparticles

Depending on the results of Cyclic Voltammetry, UV-Vis spectroscopy and transmission electron microscopy (TEM), *Aspergillus niger* NCIM 616 was found to be the better strain. Therefore, the gold nanoparticles fabricated by this strain was tested for antioxidant properties further.

A. DPPH Assay

1,1-diphenyl-2-picryl hydroxyl (DPPH) quenching assay 1 ml of 0.1 mM DPPH in ethanol was prepared. Mycofabricated gold nanoparticles (using *Aspergillus niger* NCIM 616) were added in varying concentrations (50 - 250 µg/mL) were added. The mixture was incubated for 30 minutes and the absorbance was observed at 517 nm [Rushender C.R. et. al. (2012)]. Colour changes from purple (DPPH) to yellow (DPPHH) after reduction.

DPPH• (Free radical) + AH (AuNP) = DPPHH + A•

The DPPH free radical scavenging activity was subsequently calculated as

$$\% \text{ free radical scavenging} = \frac{\text{Control OD} - \text{Sample OD}}{\text{Control OD}} \text{ x } 10$$

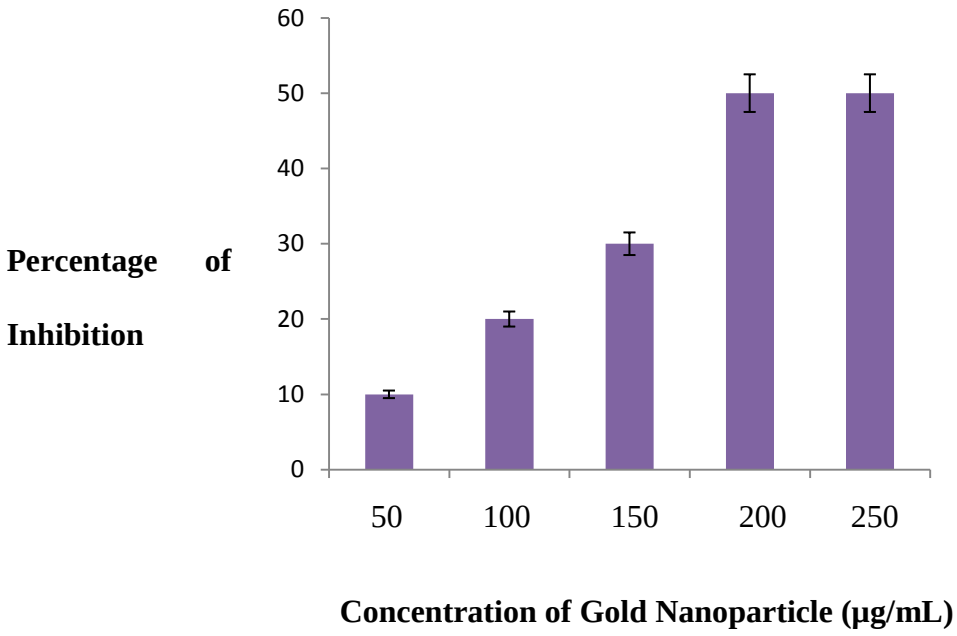

Figure 4.37: Bar-chart of Concentration of Gold Nanoparticle versus Percentage of Inhibition in DPPH Assay

B. Hydrogen Peroxide Assay

The mycofabricated gold nanoparticles (using *Aspergillus niger* NCIM 616) were added in varying concentrations (20-120 µg/mL). To that 0.6 ml of hydrogen peroxide with the already prepared phosphate buffer (pH 7.4) was added. The reaction mixture was incubated at room temperature for 10 minutes [Rushender *et al.* (2012)].

After incubation the absorbance was read at 230 nm against the blank solution with phosphate buffer.

$$\% \text{ free radical scavenging} = \frac{\text{Control OD} - \text{Sample OD}}{\text{Control OD}} \text{ x } 100$$

DPPH is a stable free radical at room temperature and accepts an electron or hydrogen radical to become stable dielectric molecules [Soares *et al.* (1997)]. The antioxidant substance donate a hydrogen atom to the DPPH free radical, thus reducing DPPH to the stable non-radical compound 1,1-diphenyl-2-picril-hydrazine. This transition is characterized by a colour change from purple to pale yellow or colourless which can quantified by its decrease absorbance at wavelength 517 nm [Amarowicz *et al.* (2004)]. The decrease in absorbance of DPPH radical caused by antioxidants, because of the reaction between antioxidant molecule and radical progresses, results in the scavenging of the radical by hydrogen donation. The total antioxidant activity of an antioxidant cannot be evaluated by using one single method, due to oxidative processes. Therefore, at least two methods should be employed in order to evaluate the total anti oxidant activity [Gulcin *et al.* (2005)]. Free radical formed in biological system are capable of damaging almost every molecule, proteins, DNA, unsaturated fatty acids and lipids in almost every biological membranes found in living cells [Labella *et al.* (1998)].

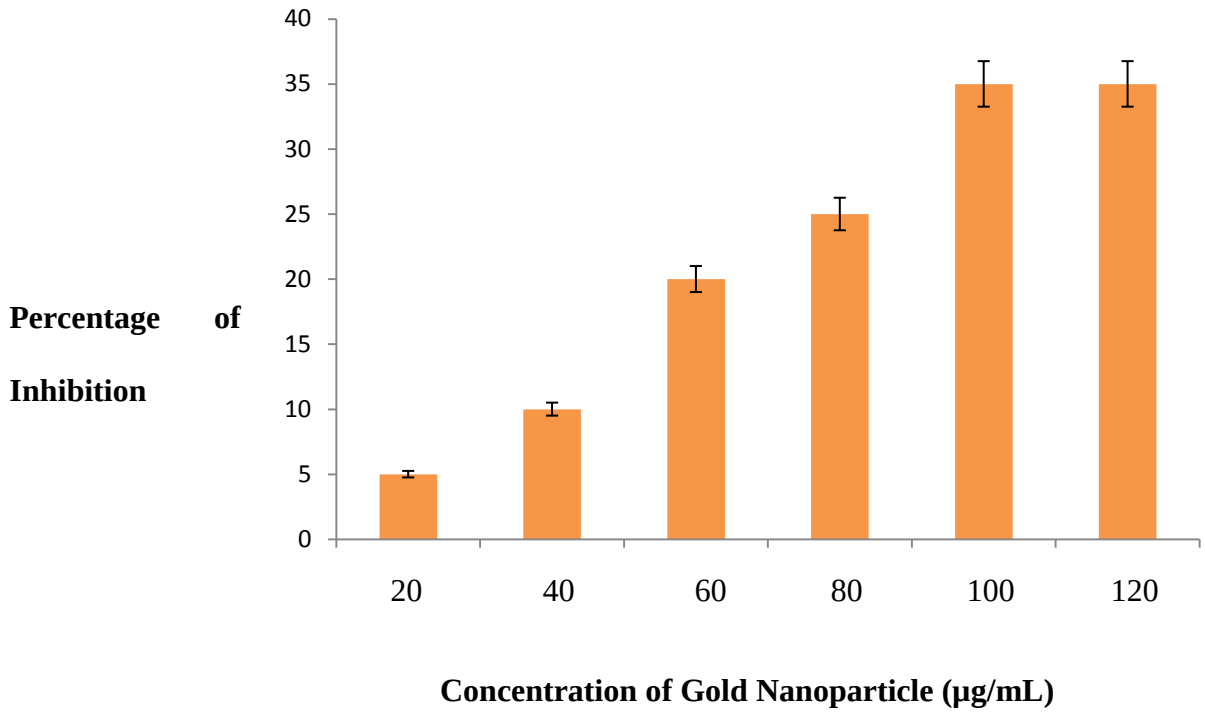

Figure 4.38: Bar-chart of Concentration of Gold Nanoparticle versus Percentage of Inhibition in Hydrogen Peroxide Assay

The mold extracts were tested in different concentrations against DPPH & hydrogen peroxide to find the radical scavenging activity (fig. 4.37 & 4.38). The antioxidant activity was found to be maximum for the 200 µg/ml of mold extract that was used in the DPPH assay and 100 µg/ml for hydrogen peroxide assay. Free radical scavenging activity of the gold nanoparticles on DPPH radicals was found to increase with increase in the concentration. These results suggests that the gold nanoparticles had good free radical scavenging capabilities.